International Journal of Advanced Engineering, Management and Science (IJAEMS)
Peer-Reviewed Journal
ISSN: 2454-1311 | Vol-11, Issue-4; Jul-Aug, 2025
Journal Home Page: https://ijaems.com/
DOI: https://dx.doi.org/10.22161/ijaems.114.9

Flexural Behavior of Strip Footing Foundations Reinforced with Uniaxial Geogrids and FGRC: Experimental Study and Empirical Correlations

E. A. El-Kasaby[1], Mohab Roshdy[2], Mahmoud Awwad[3], A. A. Abo-Shark[4]

[1]Prof. of soil mechanics and foundations, Civil Engineering Department, Benha Faculty of Engineering, Benha University, Cairo, Egypt.
[2,3,4]Lecturer, Civil Engineering Department, Benha Faculty of Engineering, Benha University, Cairo, Egypt.

Received: 01 Jun 2025; Received in revised form: 25 Jun 2025; Accepted: 02 Jul 2025; Available online: 09 Jul 2025

Abstract *— Geogrids are commonly used geosynthetic materials for soil stabilization and reinforcement of earth structures, including dams and earth walls. This study investigates the impact of using uniaxial geogrids for reinforcement in fiber glass reinforced concrete (FGRC) on the flexural behavior of strip footing foundations. The experimental research consists of testing fourteen reinforced concrete strip footings to failure under line loading. The variables in this study include the number of geogrid layers (one, two, and three), the percentage of longitudinal reinforcement and type of concrete mixture. The study reports and compares deflection, loads at each stage, stiffness, ductility, energy absorption, crack patterns, steel, concrete, and geogrid strains of the footings. The results show that using geogrid layers as a reinforcing technique effectively improves the flexural behavior of reinforced concrete footings and enhances the cracking patterns. The number of geogrid layers used in the footings significantly increases the loads at each stage and decreases the deflections of the footings. Additionally, adding fibers to reinforced concrete footings, along with geogrid layers, increases the loads at different load deflection stages. An empirical equation was correlated to establish the relationship between the moment acting on the footings and the tensile strength of geogrid reinforcement. The empirical evidence from the experiments clearly indicates a substantial enhancement in the strength resistance of geogrid-reinforced footings with FGRC compared to those reinforced with steel and normal concrete mix. This Study shows geogrids improve reinforced concrete footings and stabilize earth structures for construction industry.*

Keywords *— **Geogrids, fiber glass reinforced concrete (FGRC), strip footing foundations, reinforcement, flexural behavior, failure loads, crack patterns, ductility, strain, empirical equation, Uniaxial geogrid.***

I. INTRODUCTION

Reinforced concrete is widely used in the construction industry due to its adaptability and versatility [1]. However, the corrosion of steel reinforcements used in concrete can lead to structural deterioration and costly repairs [2]. Alternative materials such as glass, jute, synthetic coconut fibers, rubber, plastics, sisal, and hemp have been explored in various studies to improve the tensile strength of concrete [3,4]. In recent years, plastics have been under scrutiny due to their negative impact on the environment and oceans. Despite this, they are still used as strengthening components in civil infrastructure, alongside other materials [5-6].

Geogrid has been utilized as a reinforcement and stabilization material in various civil and

infrastructure works, making it a crucial component in geotechnical engineering. As an alternative to steel reinforcement, geogrid can be used to supplement or replace it and effectively reduce structural damage resulting from impact [7]. Geogrid is used in uniaxial or biaxial forms, depending on the application. Uniaxial is suitable for slope separators and retaining walls, while biaxial is best for highway structures like bridges, drainage, and pavements [8, 9]. Geogrids expand available land by allowing for the construction of steep slopes or walls, even on weak terrain. They're also used to reinforce pavements and stabilize materials in unconsolidated surfaces and asphalt layers [10-11].

Geosynthetics have long been used for reinforcement and stabilization in earthwork construction [12]. Nowadays, they're commonly used as reinforcing elements in asphalt layers [13,14] and interlayers in overlay applications [15]. However, more research is needed on their use as reinforcement in PCC overlays within pavements [16]. Uniaxial geogrids are created by elongating a polymer sheet that has been punched at regular intervals in the longitudinal direction, resulting in a higher tensile strength in the longitudinal direction compared to the transverse direction [17]. Uniaxial geogrids are commonly employed in steep slopes and retaining walls, primarily for grade separation purposes, while biaxial and triaxial geogrids find greater use in roadway applications [18].

The utilization of Geosynthetic material has significantly risen in the construction of RC and pavement structures during the past few decades. Geogrid is currently being employed in the construction of RC and pavement structures [19]. Abdel-Hay (2019) [20] found that geogrids can effectively strengthen reinforced concrete slabs as an alternative to traditional methods. Geogrids increased flexural strength and reduced deflection at failure load. The potential use of geogrids in reinforcing concrete beams has been explored by Meski and Chehab [21], as well as Hadi et al. [5]. These studies have demonstrated that geogrids can significantly enhance the strength and flexural capacity of concrete beams. Furthermore, experimental reports have indicated that the implementation of geogrids can improve the post-cracking behavior, failure mode, strength, and durability of reinforced structural members [22-23].

In recent years, there has been a growing interest in enhancing the strength of concrete through the incorporation of Glass Fiber Reinforced Concrete (GFRC) material [24]. GFRC is known for its high durability in concrete and consists of a composite material with a matrix containing an unsymmetrical dispersion or distribution of minute fibers, whether natural or artificial in origin [25]. The utilization of isolated glass fibers has been shown to increase the shear-friction strength of concrete, as well as acting as an efficient shear reinforcement. Moreover, the use of glass fibers has been found to effectively reduce crack propagation in beams [26].

This study aims to investigate the flexural behavior of strip concrete footings reinforced with geogrids. In this research, six different types of uniaxial geogrids, including both stiff and flexible options, are incorporated in the footings made of normal reinforced concrete mixture and Fiber Glass Reinforced Concrete (FGRC). The specimens are subjected to strip loading and tested under monotonic loading conditions. The experimental results demonstrate that the inclusion of geogrids in the concrete footings significantly enhances the post-cracking ductility and strength, especially in footings reinforced with multiple layers of geogrids. Furthermore, an empirical equation is derived to establish the relationship between the moment acting on the footings and the tensile strength of the geogrid reinforcement.

II. EXPERIMENTAL PROGEAM

2.1 Samples and test matrix

The experimental program involved testing fourteen specimens with varying reinforcement configurations. Each specimen had precise dimensions and loading details as follows: a length of 60 cm, a width of 30 cm, and a thickness of 9 cm, as illustrated in Figure 1. The footings were categorized into four groups to assess the effectiveness of the reinforcement and glass fiber bristles, including two control specimens reinforced with steel using reinforced concrete mix and FGRC, two specimens reinforced with three layers of uniaxial geogrid, four specimens reinforced with two layers of uniaxial geogrid, and four specimens reinforced with two

layers of uniaxial geogrid. Refer to

Table 1 for a summary of the tested specimens' configurations

Group Name	Code of Specimen	Reinforced Material	Number of Unit	Concrete Mixture
Control	St 1	Steel	3 @ 6 mm	Normal Reinforced concrete mix (Without adding fibers)
	St 8			Fiber glass reinforced concrete, FGRC (2.5 Kg/m3)
Group 1	St 2	Re 510	3 layers	Normal Reinforced concrete mix (Without adding fibers)
	St 9			Fiber glass reinforced concrete, FGRC (2.5 Kg/m3)
Group 2	St 3	Re 520	2 layers	Normal Reinforced concrete mix (Without adding fibers)
	St 10			Fiber glass reinforced concrete, FGRC (2.5 Kg/m3)
	St 4	Re 540	2 layers	Normal Reinforced concrete mix (Without adding fibers)
	St 11			Fiber glass reinforced concrete, FGRC (2.5 Kg/m3)
Group 3	St 5	Re 560	One layer	Normal Reinforced concrete mix (Without adding fibers)
	St 12			Fiber glass reinforced concrete, FGRC (2.5 Kg/m3)
	St 6	Re 570	One layer	Normal Reinforced concrete mix (Without adding fibers)
	St 13			Fiber glass reinforced concrete, FGRC (2.5 Kg/m3)
	St 7	Re 580	One layer	Normal Reinforced concrete mix (Without adding fibers)
	St 14			Fiber glass reinforced concrete, FGRC (2.5 Kg/m3)

2.2 Material properties.

The present study includes a thorough depiction of the materials utilized in our research. We provide a detailed overview of the properties of the materials used in our investigation, specifically concrete, steel fibers, and geogrids. This information aims to provide a clear understanding of the materials employed in our research and their respective characteristics.

2.2.1 Reinforced concrete materials

We utilized Ordinary Portland Cement (OPC-42.5 grade) and natural sand with a fineness modulus of 2.6, along with filter stones with a maximum aggregate size of 9 mm in our tested specimens. It was estimated that the compressive strength (f_{cu}) would reach 28 MPa at 28 days for reinforced concrete mix and 32.26 MPa for FGRC. The actual f_{cu} value was obtained on the day of testing. The concrete mix used by the FGRC had a consistent proportion of materials along with the addition of 2.5 kg/m^3 of glass fibers bristles have 12-16 mm length and 12-micron diameter CMB Group company, Egypt, Table2.

Table 2: Concrete mix content by weight for one cubic meter of concrete.

Material	Quantity
Cement (Kg/ m^3)	450
Sand (Kg/ m^3)	680
Water (Liter/ m^3)	215
Coarse aggregate (Kg/ m^3)	970
Fiber glass bristles (Kg/m^3)	2.5

2.2.2 Footing reinforcement

The control specimen of this study utilized normal mild steel bars with a 6 mm diameter and a grade of 36, which possess a yield stress of 36 Ksi, as its primary reinforcement in both directions (as depicted in Figure 1-a). In addition, uniaxial geosynthetics geogrids, manufactured by Tensar International Corporation and imported by National Geotechnical Company for GEOTECH, were utilized throughout the study (as specified in reference [27]). The mechanical properties of the uniaxial geogrids utilized in this study were documented in Table 3 and were consistent with those provided by the

manufacturer. Uniaxial Geogrids Re 510, Re520, Re540, Re560, Re570, and Re580 were employed and depicted in Figures 2-b to 2-g. Tensile strength and elongation were measured in compliance with EN ISO 10319, ASTM D6637, and GG2-87 standards.

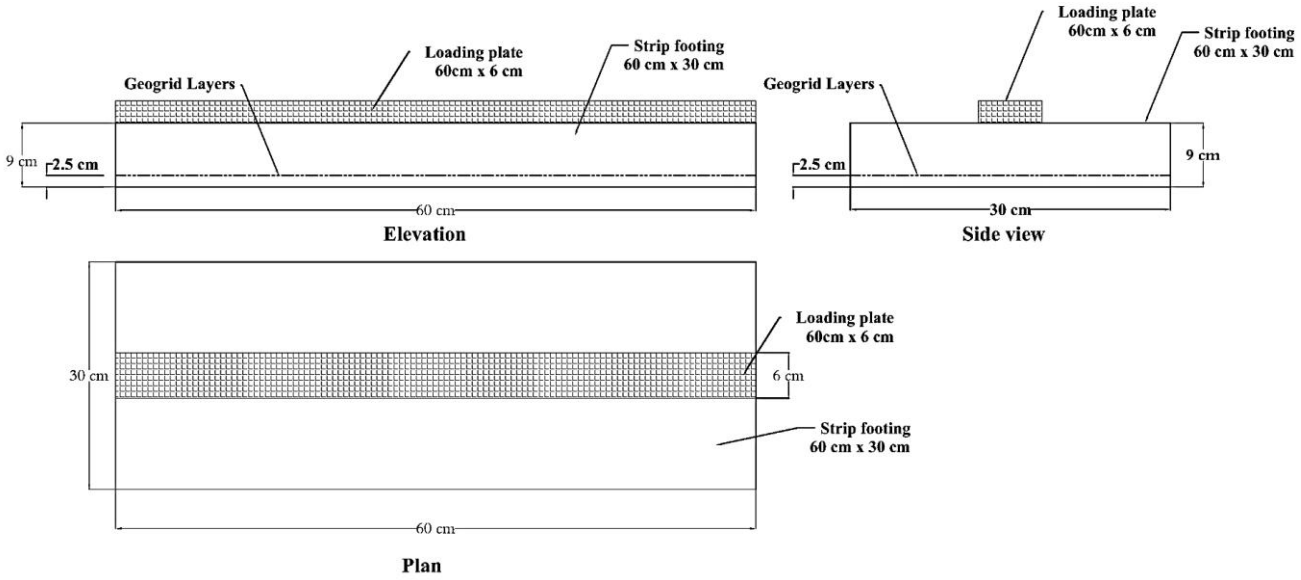

Fig.1: Specimen Dimensions and Loading Details.

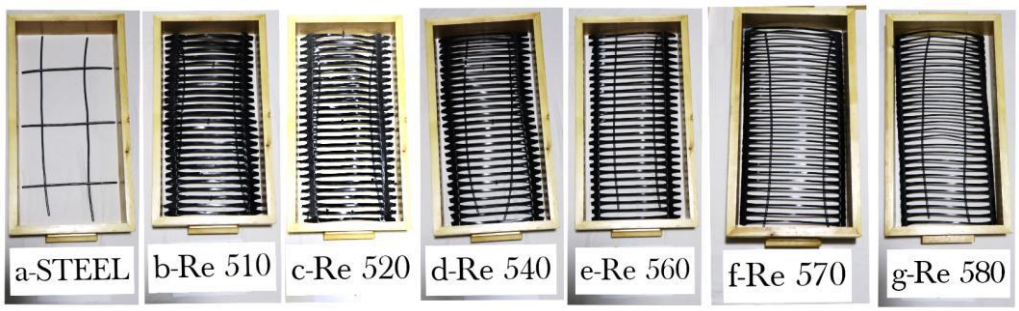

Fig. 2: Steel Bars and Uniaxial Geogrids Used in the Study

Table 3: Uniaxial Geogrid Mechanical Properties Consistent with Manufacturer's Specifications.

Mechanical properties	Component of Uniaxial geogrid						Unit
	Type of Geogrid						
	Re 510	Re 520	Re 540	Re 560	Re 570	Re 580	
polymer	High density polyethylene						-
Junction strength	95						%
Unit weight	0.29	0.36	0.45	0.65	0.87	0.98	Kg/m²
Long term strength	19.01	25.10	30.66	42.16	56.28	65.27	Kn/m

2.2.3 Analysis of Soil Specifications

The soil used in this research conforms to the well-graded gravel with sand classification based on the unified soil classification system. The uniformity coefficient and uniformity curvature, two crucial indicators for determining soil grading, were determined to be 22.50 and 1.98, respectively. Furthermore, to assess the soil's compaction characteristics, the standard proctor test, a standardized method in geotechnical engineering, was performed. The results reveal that the maximum dry density and the optimum moisture content were 2.078 t/m3 and 6.88%, respectively. These comprehensive test results and analyses are crucial in determining the soil's suitability for use under the footings. a research investigation was performed utilizing a model configuration that included a sturdy test tank. The test tank was engineered to be spacious enough to accommodate the footing without causing significant impact on the soil stresses and strains due to the tank boundaries. The dimensions of the tank were 1.50 m in length, 1.50 mm in width, and 0.70 m in height, and it was constructed from durable steel, Figure3 .

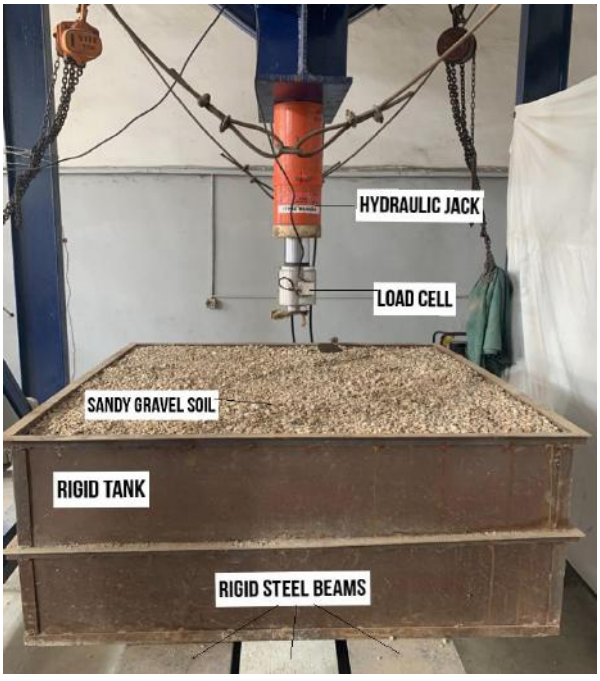

Fig. 3: Test Tank Configuration for Investigation of Footing-Soil Interaction.

2.3 Test Set-Up and Instrumentations

The samples were loaded with a hydraulic jack with a maximum capacity of 1000 (KN), linked to electric pump, and hung with a rigid reaction frame with a maximum capacity of 1000 (KN). The strip footings were placed on the compacted soil with care. It was ensured that the footings were horizontal to achieve uniform stress distribution beneath them. To ensure the consistent distribution of longitudinal load on the footings, three steel pallets with dimensions of 60 cm length, 6 cm width, and 3 cm thickness were placed on top of each strip footing. The applied vertical load was measured with a load cell with a maximum capacity of 1000 (KN) placed beneath the hydraulic jack. four Linear Variable Differential Transducer (LVDT) was installed at the upper of the footing surface to monitor displacement. All test data were collected with a data acquisition system and collected on a computer at two-second intervals. Figure 4 depicts the test setup which was applied in the concrete laboratory of Benha Faculty of Engineering at the University of Benha.

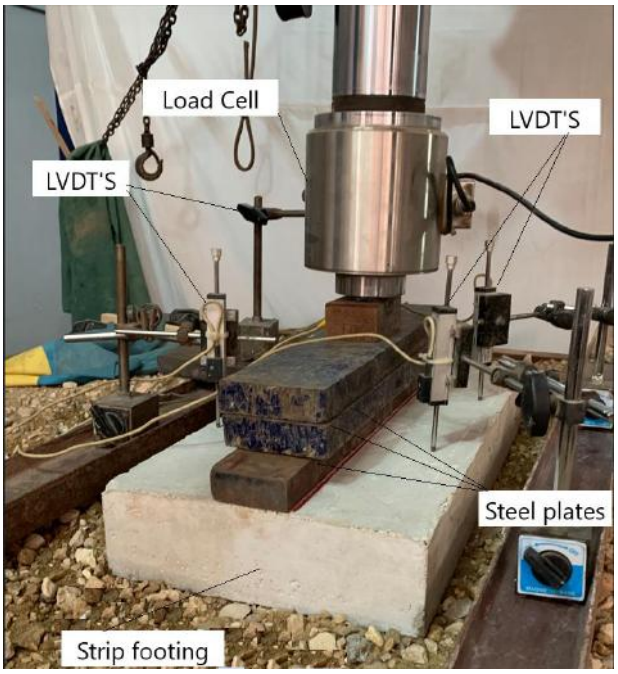

Fig. 4: Experimental Setup for strip footings

III. EXPERIMENTAL RESULTS AND DISCUSSION

3.1 General

An organizational chart has been included to streamline the presentation of the analysis of experimental strip footing results. This chart serves as a visual guide, simplifying the structure of the

analysis by breaking down its various components and findings, Fig. 5.

Fig. 6 illustrates the load-deflection behavior of strip concrete footings reinforced with one, two, and three layers of uniaxial geogrids. The load-bearing capacity (P), vertical displacement (Δ), and stiffness (K) were computed for all investigated footings at the first crack, yield, and ultimate stages based on the aforementioned figures. Additionally, the ductility (μ) and energy absorption (En) characteristics of each footing were determined and are presented in Table 4.

The experimental results indicate that incorporating uniaxial geogrids in strip footings resulted in superior load-deflection behavior compared to steel-reinforced footings. This outcome could be attributed to the comparable tensile strength of uniaxial geogrids to that of steel, while exhibiting unique mechanical properties. The longitudinal placement of uniaxial geogrids at closely spaced intervals within the strip footing, in conjunction with the strong bonding between the concrete and geogrid sections, played a pivotal role in enhancing the load-bearing capacity of the foundation.

3.2 Geogrid's Effect on Strip Footing Performance.

The load - deflection curves of reinforced strip footings are presented in Fig. 6. Results show excellent repeatability of the tests, as well as the increase in peak load of reinforced concrete footings with geogrid compared to reinforced concrete footing with steel, Table 4.

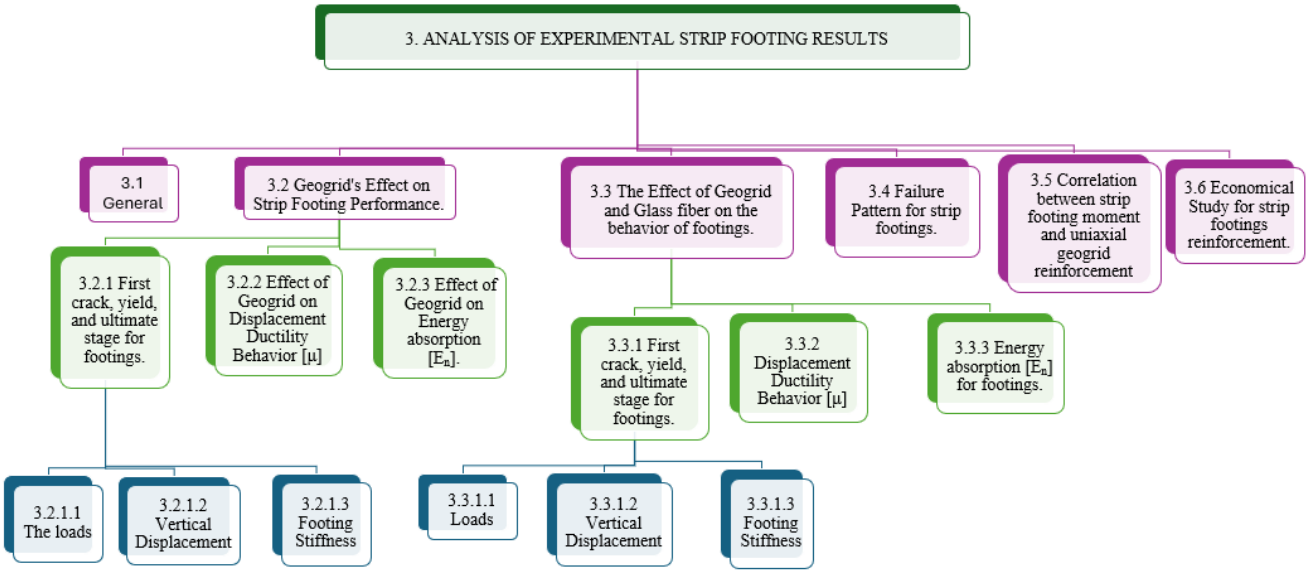

Fig. 5: Organizational Chart for Analysis of Experimental strip Footing Results.

Table 4: Characteristics of Reinforced Strip Concrete Footings.

	First crack stage			Yield stage			Ultimate load stage			Ductility factor (μ)	Energy absorption (kN/mm)
	P_f (kN)	Δ_f (mm)	K_f (kN/mm)	P_y (kN)	Δ_y (mm)	K_y (kN/mm)	P_u (kN)	Δ_u (mm)	K_u (kN/mm)		
St1	90.000	15.600	5.769	101.500	18.130	5.598	112.013	23.310	4.805	1.286	1413.855
St2	106.000	11.900	8.908	170.253	27.253	6.247	192.030	40.902	4.695	1.501	5516.970
St3	96.500	11.300	8.540	146.444	23.816	6.149	162.660	34.177	4.759	1.435	3758.603
St4	112.000	12.920	8.669	196.514	28.700	6.847	216.971	43.270	5.014	1.508	6313.279
St5	95.000	14.323	6.633	127.975	23.632	5.415	135.853	26.868	5.056	1.137	2115.115
St6	100.000	12.600	7.937	156.323	24.995	6.254	177.808	36.060	4.931	1.443	4268.647
St7	114.000	13.000	8.769	208.199	30.032	6.933	224.263	45.954	4.880	1.530	7008.947

St8	96.000	13.960	6.877	107.500	16.533	6.502	115.988	23.113	5.018	1.398	1674.911
St9	111.000	11.620	9.552	175.848	25.082	7.011	203.349	41.905	4.853	1.671	5898.083
St10	105.000	13.250	7.925	150.807	22.284	6.767	170.116	34.392	4.946	1.543	3936.992
St11	124.000	12.320	10.065	199.997	26.650	7.505	220.216	45.589	4.830	1.711	6887.856
St12	102.000	14.180	7.193	132.024	22.013	5.998	143.395	27.808	5.157	1.263	2437.114
St13	110.000	12.700	8.661	163.127	24.056	6.781	188.208	38.631	4.872	1.606	4840.592
St14	128.000	11.800	10.847	215.139	28.051	7.670	230.979	48.089	4.803	1.714	7966.644

Results of reinforced concrete footings with steel show that specimens failed in a brittle mode immediately after peak, reaching peak loads of 112 and 115.9 kN at failure for St1 and St8. On the other hand, the load-deformation curves of reinforced concrete specimens with geogrid exhibited delayed failure and extra peak load in all cases. After load drop, reinforced geogrid footings gained post cracking ductility until cracks reached top surface footings, where failure was completed.

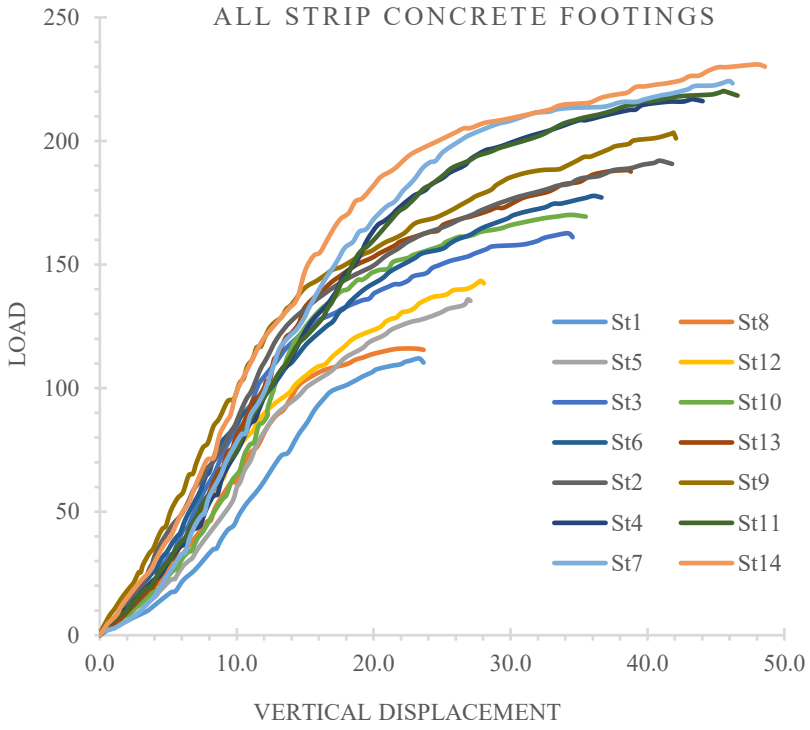

Fig. 6: Load-deflection behavior of reinforced strip concrete footings.

At this point, each specimen was compared to its control in order to extract the influence of the geogrid's presence within the footings independently. The following variables have been investigated:

3.2.1 Effect of Geogrid on First crack, Yield and Ultimate stages for footings.

The findings of this study revealed that the incorporation of geogrid reinforcement in the footings resulted in delayed initiation of initial cracks, and the post-cracking behavior of the reinforced footings exhibited higher load-carrying capacities than the control footings.

3.2.1.1 The Loads

In comparison to control footings, the use of uniaxial geogrid reinforcement resulted in gradual increases in the values of the cracking load (P_{fc}), yield load (P_y), and ultimate load (P_{ult}), Fig. 7. These results demonstrate the effectiveness of geogrid reinforcement in enhancing the load-carrying capacity of reinforced concrete footings, as follows:

- P_{fc}, P_y and P_{ult} values at footings reinforced by Three layers of uniaxial geogrid Re 510 increases by about average 16.70%,65.65% and 73.37% respectively than that for relative control footing.
- P_{fc}, P_y and P_{ult} values at footings reinforced by two layers of uniaxial geogrid Re 520 increases by about average 8.29%,42.28% and 45.94% respectively than that for relative control footing.
- P_{fc}, P_y and P_{ult} values at footings reinforced by two layers of uniaxial geogrid Re 540 increases by about average 26.80%,89.82% and 91.78% respectively than that for relative control footing.
- P_{fc}, P_y and P_{ult} values at footings reinforced by one layer of uniaxial geogrid Re 560 increases by about average 5.90%,24.44% and 22.45% respectively than that for relative control footing.
- P_{fc}, P_y and P_{ult} values at footings reinforced by one layer of uniaxial geogrid Re 570 increases by about average 12.84%,52.87% and 60.50% respectively than that for relative control footing.
- P_{fc}, P_y and P_{ult} values at footings reinforced by one layer of uniaxial geogrid Re 580 increases by about average 30.00%,102.62% and 99.67% respectively than that for relative control footing.

The incorporation of uniaxial geogrid reinforcement into strip footing yields substantial enhancements in load-bearing capacities. On average, P_{fc}, P_y, and P_{ult} increase by approximately 16.75%, 62.94%, and 65.61% respectively Compared to relative control footing. With respect to the tensile strength of uniaxial reinforcement into the strip footing.

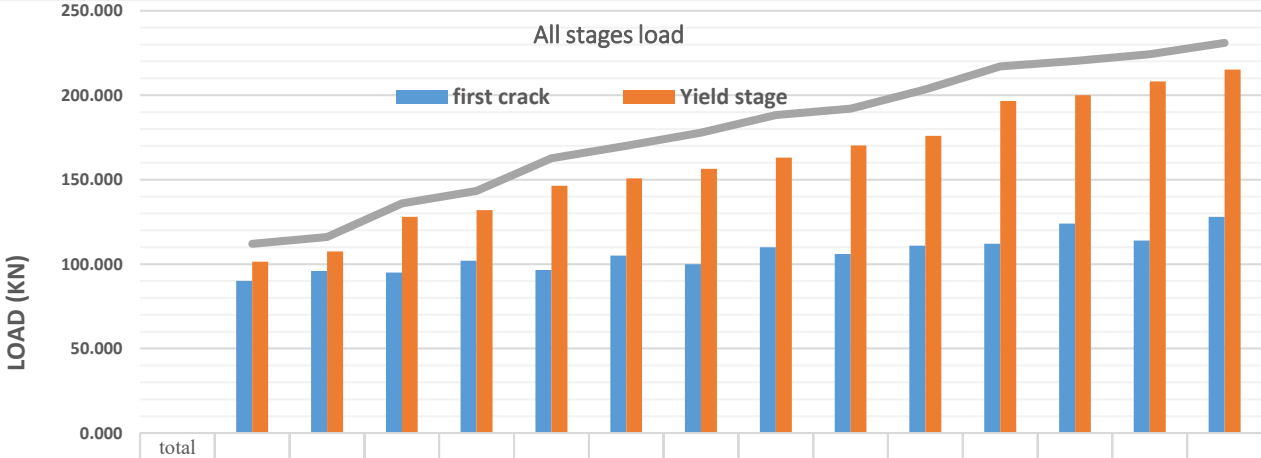

SPECIFICATIONS OF FOOTINGS														
	total tensile strength	25.440	25.440	25.290	25.290	30.120	30.120	33.760	33.760	34.200	34.200	36.780	36.780	39.160	39.160
	Footing number	s1	s8	s5	s12	s3	s10	s6	s13	s2	s9	s4	s11	s7	s14
first crack		90.000	96.000	95.000	102.000	96.500	105.000	100.000	110.000	106.000	111.000	112.000	124.000	114.000	128.000
Yield stage		101.500	107.500	127.975	132.024	146.444	150.807	156.323	163.127	170.253	175.848	196.514	199.997	208.199	215.139
ultimate stage		112.013	115.988	135.853	143.395	162.660	170.116	177.808	188.208	192.030	203.349	216.971	220.216	224.263	230.979

Fig. 7: Quantification of Load Magnitudes at Each Stage for Multiple Footing Types.

3.2.1.2 Vertical Displacement

Based on the obtained results, it can be inferred that.

- Δ_{fc} values at footings reinforced by Three layers of uniaxial geogrid Re 510 decreases by about average 20.24% than that for relative control footing. while, Δ_y and Δ_{ult} increases by about 51.01% and 78.38% respectively than that for relative control footing.
- Δ_{fc} values at footings reinforced by two layers of uniaxial geogrid Re 520 decreases by about average 16.32% than that for relative control footing. while, Δ_y and Δ_{ult} increases by about 33.07% and 47.70% respectively than that for relative control footing.
- Δ_{fc} values at footings reinforced by two layers of uniaxial geogrid Re 540 decreases by about average 14.46% than that for relative control

footing. while, Δ_y and Δ_{ult} increases by about 59.74% and 91.43% respectively than that for relative control footing.

- Δ_{fc} values at footings reinforced by one layer of uniaxial geogrid Re 560 decreases by about average 3.30% than that for relative control footing. while, Δ_y and Δ_{ult} increases by about 31.74% and 17.78% respectively than that for relative control footing.
- Δ_{fc} values at footings reinforced by one layer of uniaxial geogrid Re 570 decreases by about average 14.12% than that for relative control footing. while, Δ_y and Δ_{ult} increases by about 41.68% and 60.91% respectively than that for relative control footing.
- Δ_{fc} values at footings reinforced by one layer of uniaxial geogrid Re 580 decreases by about average 16.07% than that for relative control footing. while, Δ_y and Δ_{ult} increases by about 67.65% and 102.60% respectively than that for relative control footing.

Compared to a control footing, uniaxial geogrid reinforcement typically increases the values of vertical displacement at the yield stage (Δ_y) and ultimate stage (Δ_{ult}), while decreasing the displacement at the cracking stage (Δ_{fc}), as observed in the load-deflection curves as follows.

3.2.1.3 Footing Stiffness

When compared to a control foundation, the use of uniaxial geogrid reinforcement typically results in gradual increases in the stiffness values at the cracking stage (k_{fc}) and yield stage (k_y), while there is a decrease in stiffness at the ultimate stage (k_{ult}). This behavior was observed as the predominant characteristic of the specimens. The results of the study are summarized as follows:

- K_{fc} and K_y values at footings reinforced by Three layers of uniaxial geogrid Re 510 increases by about average 46.65% and 9.70 % respectively than that for relative control footing. While K_{ult} decreases by about 2.79% compared to that for relative control footing.
- K_{fc} and K_y values at footings reinforced by two layers of uniaxial geogrid Re 520 increases by about average 31.63% and 6.95 % respectively than that for relative control footing. While K_{ult} decreases by about 1.19% compared to that for relative control footing.
- K_{fc} , K_y and K_{ult} values at footings reinforced by two layers of uniaxial geogrid Re 540 increases by about average 48.30% ,18.86 % and 0.30% respectively than that for relative control footing.
- K_{fc} and K_{ult} values at footings reinforced by one layer of uniaxial geogrid Re 560 increases by about average 9.78% and 3.98 % respectively than that for relative control footing. While K_y decreases by about 5.51% than that for relative control footing.
- K_{fc} and K_y values at footings reinforced by one layer of uniaxial geogrid Re 570 increases by about average 31.75% and 8.00 % respectively than that for relative control footing. While K_{ult} decreases by about 0.15% than that for relative control footing.
- K_{fc} and K_y values at footings reinforced by one layer of uniaxial geogrid Re 580 increases by about average 54.87% and 20.89 % respectively than that for relative control footing. While K_{ult} decreases by about 1.36% compared to that for relative control footing.

In the majority of cases, a notable enhancement in Footing Stiffness was observed during the initial and yield stages, followed by a subsequent decline in Stiffness values as the strip footings progressed to the ultimate stage. This pattern underscores the significant influence of the uniaxial geogrid on the early stages of strip footing stiffness. However, it's noteworthy that the stiffness gains seem to diminish once the uniaxial geogrid sheets experience elongation, leading to a vulnerability and weakening of the specimens.

3.2.2 Effect of geogrid on Displacement Ductility Behavior [μ]

In this study, we evaluated the effect of geogrid reinforcement on the displacement ductility behavior of concrete footings. The displacement ductility index, which represents the ability of the structural element to undergo large deflections without significant strength reduction before failure, was used to assess the performance of the concrete footings. To ensure concrete structures can withstand seismic events, they must maintain their strength above the yield strength up to the allowable plastic deformation adopted in the design.

Our findings demonstrate that the incorporation of geogrid reinforcement can significantly enhance the displacement ductility behavior of concrete footings. The displacement ductility indexes of the geogrid-reinforced footings were 18.11% higher for group 1, which had 3 layers of uniaxial geogrid, 11% to 19.8% higher for group 2, which had 2 layers of uniaxial geogrid, and 13.5% to 20.8% higher for group 3, which had 1 layer of uniaxial geogrid, compared to the control footings.

Our study also revealed a positive correlation between the increase in displacement ductility and the stiffness with tensile strength of the uniaxial geogrids used. Moreover, increasing the number of geogrid layers did not negatively affect the behavior of the footings, as observed in the load-deflection curves.

Therefore, incorporating multiple layers of uniaxial geogrid reinforcement can be a practical and effective solution for improving the performance of reinforced concrete footings in many conditions. These results have significant implications for the design of reinforced concrete structures in earthquake-prone regions, Fig. 8, depicts the relationship between the tensile strength of geogrid reinforcement and the corresponding increase in ductility factor ratio for footing specimen. The data in the figure shows a clear trend of increasing ductility factor ratio with increasing tensile strength of the geogrid reinforcement.

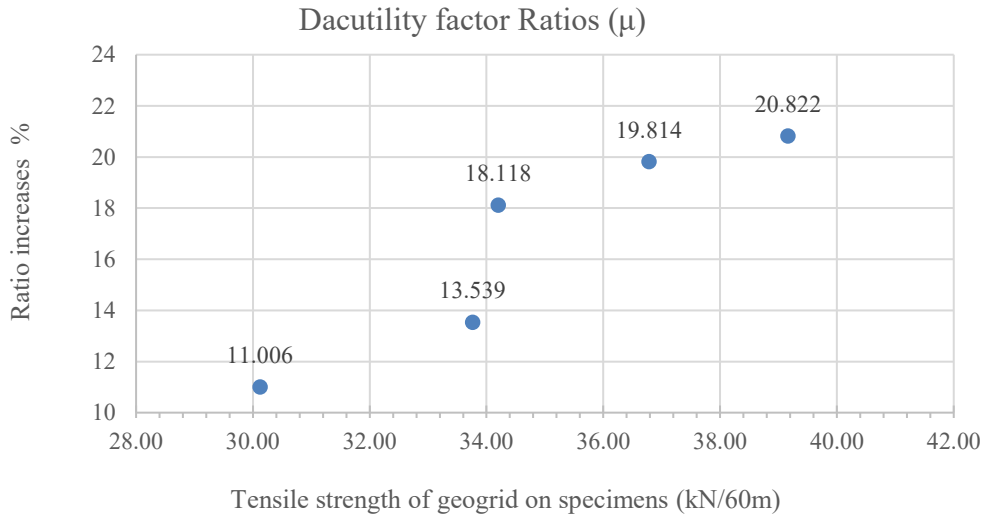

Fig. 8: Relationship between the tensile strength of geogrid reinforcement and the corresponding increase in ductility factor ratio for footings.

Uniaxial Geogrid reinforcement substantially enhances concrete footing displacement ductility. On average, geogrids exhibit an improvement of 11% to 20.82% compared to relative control footings. Depending on geogrid tensile strength of footing reinforcement.

3.2.3 Effect of Geogrid on Energy absorption [E_n] for footings.

A high capacity for energy absorption is beneficial in the event of major earthquakes, where substantial energy dissipation is necessary to prevent significant dynamic responses and hysteretic damping in concrete structures. The energy absorption capacity of the tested footings was determined by calculating the area enclosed by their load-deflection curves.

In addition, the behavior of the tested footings was compared based on their energy absorption capacity, which was determined by calculating the area under their load-deflection curves, Fig. 6. The energy dissipation capacities were increased by a percent varying from 42.55% to 385.69% for all groups of uniaxial geogrid reinforcement compared to the concrete control footing "St1 and St8" with a positive correlation to the stiffness and tensile strength of geogrid.

Moreover, increasing the number of geogrid layers did not negatively affect the behavior of the footings, as observed in the result obtained, Fig. 9, depicts the relationship between the tensile strength of geogrid reinforcement and the corresponding increase in energy absorption ratio for strip footings specimen.

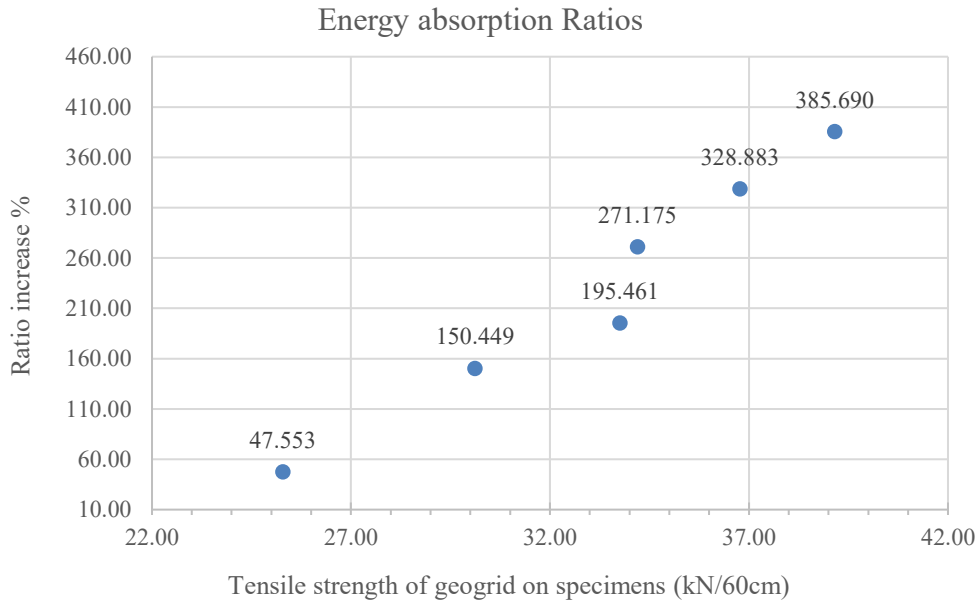

Fig. 9: Relationship between the tensile strength of geogrid reinforcement and the corresponding increase in energy absorption ratio for footings.

The Energy dissipation capacities increased by a percent varying from 42.55% to 385.69% for uniaxial geogrid reinforcement compared to relative control footings with a positive correlation to the stiffness and tensile strength of geogrid.

3.3 The Effect of Geogrid and Glass Fiber on the behavior of footings.

3.3.1 First crack, Yield, and Ultimate stage for footings

It was found that the reinforcement footings by glass fiber and geogrid would delay the onset of initial cracks and the post-crack behavior of the reinforcement footings demonstrated higher load-carrying capacities than the strip footing (St1), Fig 10.

3.3.1.1 The Loads

As compared to a control strip footing, uniaxial geogrid reinforcing with (GFRC) often results in gradual increases in the values of the cracking load (P_{fc}), yield load (P_y), and ultimate load (P_{ult}) as follows:

- P_{fc}, P_y and P_{ult} values at footings reinforced by Three layers of uniaxial geogrid Re 510 increases by about average 23.33%,73.24% and 81.540% respectively than for the concrete control footing (St1).
- P_{fc}, P_y and P_{ult} values at footings reinforced by two layers of uniaxial geogrid Re 520 increases by about average 16.66%,48.57% and 51.87% respectively than for the concrete control footing (St1).
- P_{fc}, P_y and P_{ult} values at footings reinforced by two layers of uniaxial geogrid Re 540 increases by about average 37.77%,97.04% and 96.59% respectively than for the concrete control footing (St1).
- P_{fc}, P_y and P_{ult} values at footings reinforced by one layer of uniaxial geogrid Re 560 increases by about average 13.33%,30.07% and 28.06% respectively than for the concrete control footing (St1).
- P_{fc}, P_y and P_{ult} values at footings reinforced by one layer of uniaxial geogrid Re 570 increases by about average 22.22%,60.71% and 68.02% respectively than for the concrete control footing (St1).
- P_{fc}, P_y and P_{ult} values at footings reinforced by one layer of uniaxial geogrid Re 580 increases by about

average 42.22%,111.96% and 106.20% respectively than for the concrete control footing (St1).

Glass fiber bristles with Uniaxial geogrid reinforcement, particularly with Re 510, Re 520, Re 540, Re 560, Re 570, and Re 580, consistently enhances strip footing performance, yielding increases of approximately 13.33% to 42.22% for P_{fc}, 30% to 111.96% for P_y, and 28.06%, to 106.20% for P_{ult} compared to the concrete control strip footing (St1).

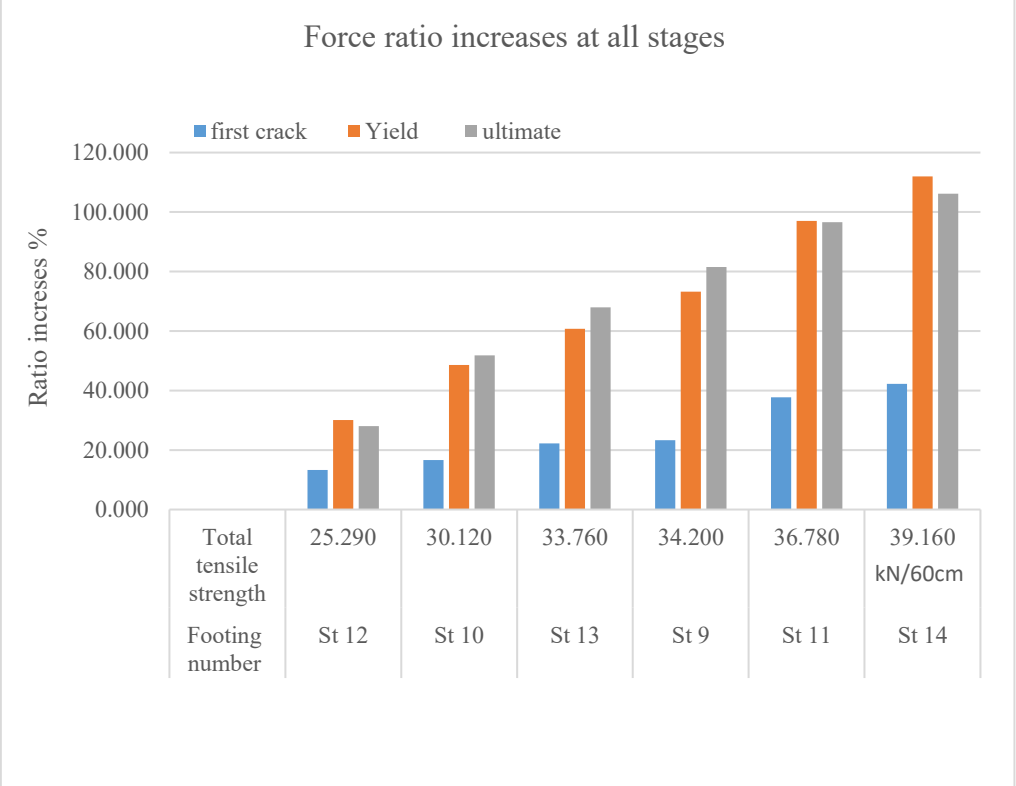

Fig. 10: Percentage Enhancement of specimen force Ratios with total tensile strength of geogrid Compared to Control specimen (St1).

3.3.1.2 Vertical Displacement

Based on the obtained results, it can be inferred that.

- Δ_{fc} values at footings reinforced by Three layers of uniaxial geogrid Re 510 decreases by about average 25.51% than that for the concrete control footing (St1). while, Δ_y and Δ_{ult} increases by about 38.34% and 79.77% respectively than that for the concrete control footing (St1).
- Δ_{fc} values at footings reinforced by two layers of uniaxial geogrid Re 520 decreases by about average 15.04% than that for the concrete control footing (St1). while, Δ_y and Δ_{ult} increases by about 22.91% and 47.54% respectively than that for the concrete control footing (St1).
- Δ_{fc} values at footings reinforced by two layers of uniaxial geogrid Re 540 decreases by about average 21.02% than that for the concrete control footing (St1). while, Δ_y and Δ_{ult} increases by about 46.99% and 95.57% respectively than that for the concrete control footing (St1).
- Δ_{fc} values at footings reinforced by one layer of uniaxial geogrid Re 560 decreases by about average 9.10% than that for the concrete control footing (St1). while, Δ_y and Δ_{ult} increases by about 21.41% and 19.29% respectively than that for the concrete control footing (St1).
- Δ_{fc} values at footings reinforced by one layer of uniaxial geogrid Re 570 decreases by about average 18.59% than that for the concrete control footing (St1). while, Δ_y and Δ_{ult} increases by about 32.68% and 65.72% respectively than that for the concrete control footing (St1).
- Δ_{fc} values at footings reinforced by one layer of uniaxial geogrid Re 580 decreases by about average 24.35% than that for the concrete control footing (St1). while, Δ_y and Δ_{ult} increases by about

54.71% and 106.30% respectively than that for the concrete control footing (St1).

Compared to a control footing (St1), footings reinforced by uniaxial geogrid and glass fiber bristles typically increases the values of vertical displacement at the yield stage (Δ_y) and ultimate stage (Δ_{ult}), while decreasing the displacement at the cracking stage (Δ_{fc}).

3.3.1.3 Footing Stiffness

When compared to a control foundation (St1), footings reinforced by uniaxial geogrid and glass fiber bristles typically results in gradual increases in the stiffness values at the cracking stage (k_{fc}) , yield stage (k_y) and ultimate stage (k_{ult}). This behavior was observed as the predominant characteristic of the specimens. The results of the study are summarized as follows:

- K_{fc} , K_y and K_{ult} values at footings reinforced by Three layers of uniaxial geogrid Re 510 increases by about average 65.57% , 25.22 % and 0.9 % respectively than that for the concrete control footing (St1).
- K_{fc} , K_y and K_{ult} values at footings reinforced by two layers of uniaxial geogrid Re 520 increases by about average 37.35% , 20.88 % and 2.93 % respectively than that for the concrete control footing (St1).
- K_{fc} , K_y and K_{ult} values at footings reinforced by two layers of uniaxial geogrid Re 540 increases by about average 74.45% , 34.04 % and 0.52 % respectively than that for the concrete control footing (St1).
- K_{fc} , K_y and K_{ult} values at footings reinforced by one layer of uniaxial geogrid Re 560 increases by about average 24.68% , 7.13 % and 7.30 % respectively than that for the concrete control footing (St1).
- K_{fc} , K_y and K_{ult} values at footings reinforced by one layer of uniaxial geogrid Re 570 increases by about average 50.13% , 21.12 % and 1.38 % respectively than that for the concrete control footing (St1).
- K_{fc} and K_y values at footings reinforced by one layer of uniaxial geogrid Re 580 increases by about average 88.02% and 36.99 % respectively than that for the concrete control footing (St1). While K_{ult} decreases by about 0.05% than that for the concrete control footing (St1).

Incorporating glass fiber bristles along with uniaxial geogrid reinforcement uniformly increases the stiffness of strip footing performance. This approach yields notable enhancements ranging from 24.68% to 88.02% for P_{fc}, 7.13% to 36.99% for P_y, and 0.52% to 7.3% for P_{ult} in comparison to the concrete control strip footing (St1).

3.3.2 Effect of Geogrid and Glass Fibers on Displacement Ductility Behavior [μ]

The results of the study revealed that the incorporation of uniaxial geogrid reinforcement led to a significant enhancement in the displacement ductility indexes across all experimental groups. The observed increase in these indexes ranged from 20% to 33.3% when compared to the control footing labeled as "St1." Importantly, this enhancement exhibited a positive correlation with the total tensile strength of the uniaxial geogrid reinforcement utilized, Fig. 11.

Additionally, a specific case worth noting is the group labeled as "St12," which exhibited a relatively smaller increase in displacement ductility index, amounting to a percent of 1.74%. This modest improvement can be attributed to the utilization of a lower tensile strength reinforcement, specifically measured at 25.44 kN / 60 cm.

3.3.3 Effect of Geogrid and Glass Fibers on Energy absorption [E_n] for footings.

The results of the study demonstrate a significant increase in energy dissipation capacities when using uniaxial geogrid reinforcement compared to the concrete control footing "St1." The energy dissipation capacities were found to vary between 72.37% and 463.47% for all groups of uniaxial geogrid reinforcement.

Furthermore, the study indicates a positive correlation between the tensile strength of the uniaxial geogrids and the enhanced energy dissipation capacities. This suggests that geogrids with higher tensile strength tend to exhibit greater energy dissipation capabilities.

These findings are supported by the data presented in Fig. 12, which visually represents the relationship between the energy dissipation capacities

and the different groups of uniaxial geogrid reinforcement. The figure likely illustrates the trend of increasing energy dissipation as the tensile strength of the geogrids increases.

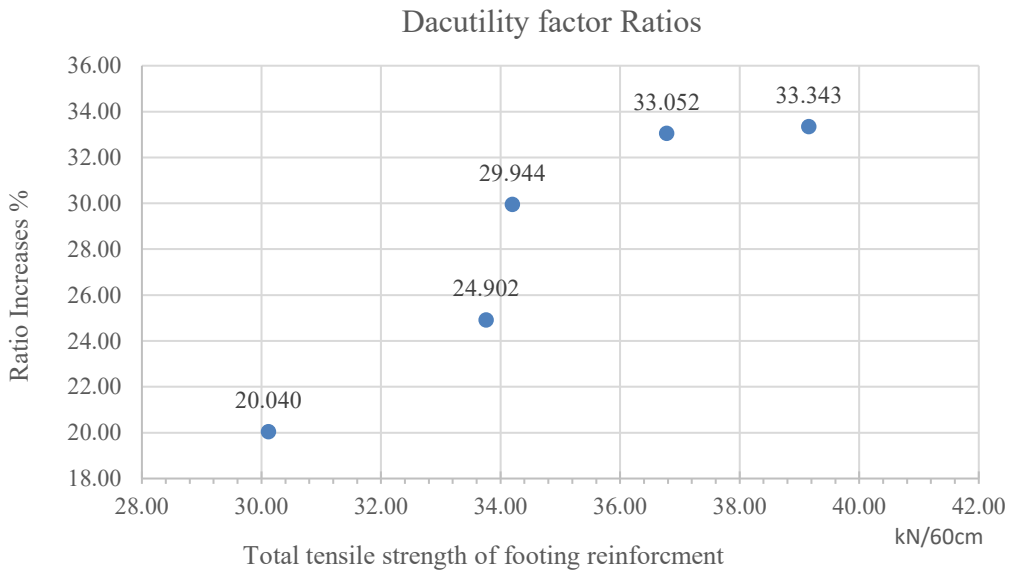

Fig. 11: Ratio of Increases in Ductility factor for strip Concrete Footings Compared to Control Footing (St1).

The study demonstrates that integrating uniaxial geogrid reinforcement with glass bristles on strip footings yields notable increases 20% to 33.3% in displacement ductility indexes across experimental groups, with a positive correlation to the total tensile strength of the reinforcement.

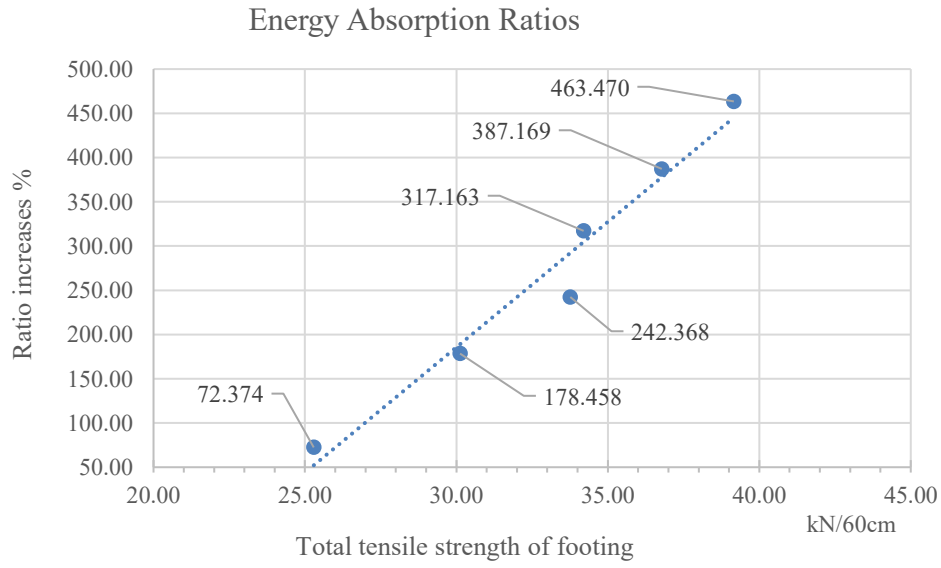

Fig. 12: Ratio of Increases in Energy Absorption for strip Concrete Footings Compared to Control Footing (St1).

The study showcases a substantial rise in energy dissipation capacities (72.37% to 463.47%) through uniaxial geogrid reinforcement compared to the concrete control footing, accentuating a direct link between geogrid tensile strength and heightened energy dissipation capabilities.

3.4 Failure Pattern For Strip Footing

In all concrete footings, cracks occurred only parallel to the load plate, resulting in flexural cracks without any shear cracks. The failure of the concrete footings was characterized by the widening of cracks, the formation of additional cracks in some footings, and the extension of these cracks from the tension zone "concrete bottom surface" to the compression zone "concrete top surface" until failure. Fig. 13, provides a visual representation of the crack patterns observed in the footings. After the footings failed, the cracks were examined to assess the condition of the geogrids' ribs. Fig. 14, displays examples of the geogrids' ribs after the failure of the concrete footings.

For the first and second case studies "group number one and two", no cutting of the uniaxial geogrids' ribs was observed. However, in the third case study "group number three", cutting was observed in most of the uniaxial geogrids' ribs.

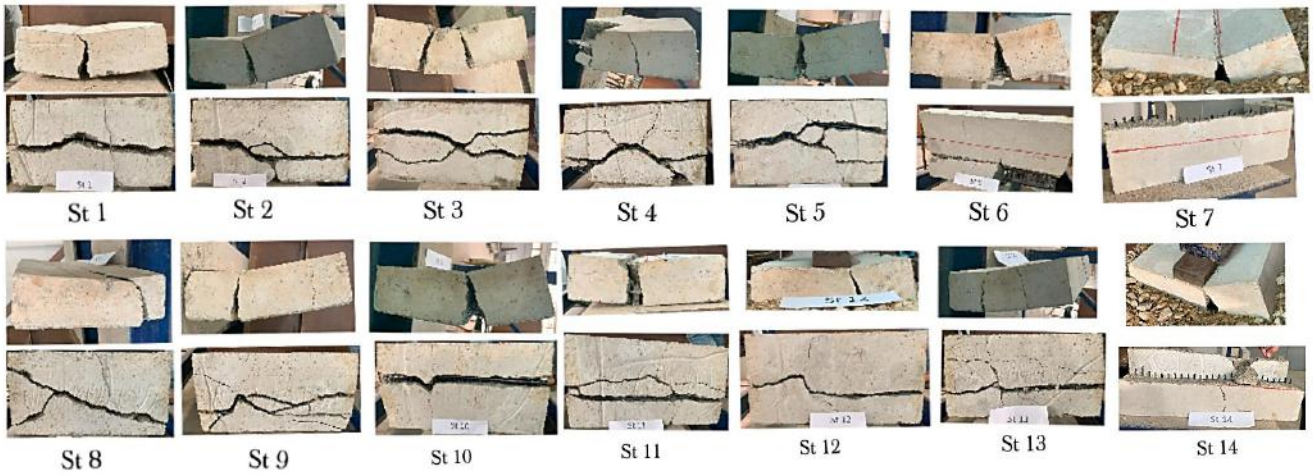

Fig. 13 : Crack Patterns in Strip Concrete Footings (illustrating the cracks observed in the footings).

Fig. 14: Geogrids' Rib Status after Failure of Concrete Footings "showing the condition of geogrids' ribs following the failure of the footings".

Among the control concrete footings St1 and St8, only one crack formed and gradually increased until failure. Similarly, for group number one "concrete footings St2 and St9", only one crack formed and increased gradually until failure. In group number two, concrete footings St3 and St10 exhibited two

parallel cracks at the point of maximum moment. In contrast, concrete footings St4 and St11 had one crack that increased gradually, accompanied by a group of small cracks parallel and perpendicular to the main crack, but not reaching the surface.

For group number three, which consisted of concrete footings St3 to St7 and St12 to St14 with one layer of geogrid, one crack formed and increased gradually until failure. These cracks were significantly thick and indicated substantial damage. They appeared both parallel and perpendicular to the original crack. Moreover, most of the specimens in this group experienced cuts in the geogrid layer, leading to their division into separate parts for further analysis and evaluation.

Therefore, a positive correlation can be observed between the number of flexural cracks, the tensile strength of geogrids, and the number of geogrid layers.

3.5 Correlation between strip footing moment and uniaxial geogrid reinforcement.

A comprehensive analysis is conducted to examine the correlation between strip footing moment and the implementation of uniaxial geogrid reinforcement. The research aims to explore the relationship between the applied moment on a strip footing and the effectiveness of using uniaxial geogrids as reinforcement. By analyzing various factors such as load distribution, soil characteristics, and geogrid properties, this study seeks to provide valuable insights into the performance and behavior of strip footings when reinforced with uniaxial geogrids. The findings of this analysis will contribute to a better understanding of the interaction between footing moments and geogrid reinforcement, aiding in the development of more efficient and reliable geotechnical design practices.

The calculation of the ultimate moment (Mu) and the required area of geogrid (Ag) for all groups of footings has yielded conclusive results and were presented on Table 5. To establish a correlation between the ultimate moment (Mu) and the required area of geogrid (Ag) for different strip footings (St 1 to St 7 for Reinforced concrete mixture and St 8 to St 14 for fiber glass reinforced concrete, FGRC), data-fit software was employed. This software allowed for the analysis of the relationship between Mu and Ag. The findings are presented in Fig. 15. Consequently, an empirical formula can be derived from these results, Eq (1).

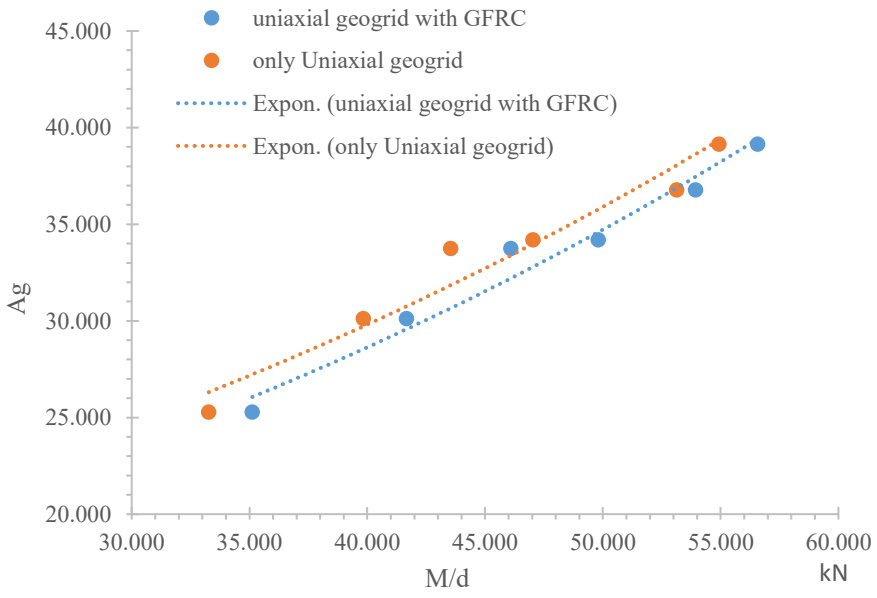

Fig. 15: Correlation between Ultimate Moment (Mu) and Required Area of Geogrid (Ag) for Different strip footings.

Table 5 : Calculations of (M/d) and (Ag) for the studied strip footing specimens.

Footing specimen No.		Ultimate Moment				M/d	Geogrid			
		p_{ult} [kN]	P_{ult} [kN/0.6 m]	$F_{act} = P_{ult} / A_{footing}$ kN/m2	$M = F_{act}*L*(c^2/2)$ kN. 0.60 m		N	L	T_{ult}	A g
Rc. mix	s5	135.853	226.421	754.738	2.994	33.271	1.000	0.600	42.150	25.290
	s3	162.660	271.101	903.669	3.585	39.837	2.000	0.600	25.100	30.120
	s6	177.808	296.346	987.821	3.919	43.546	1.000	0.600	56.267	33.760
	s2	192.030	320.050	1066.834	4.233	47.030	3.000	0.600	19.000	34.200
	s4	216.971	361.618	1205.393	4.782	53.138	2.000	0.600	30.650	36.780
	s7	224.263	373.772	1245.908	4.943	54.924	1.000	0.600	65.267	39.160
GFRC. mix	s12	143.395	238.991	796.637	3.161	35.118	1.000	0.600	42.150	25.290
	s10	170.116	283.527	945.090	3.750	41.663	2.000	0.600	25.100	30.120
	s13	188.208	313.681	1045.603	4.148	46.094	1.000	0.600	56.267	33.760
	s9	203.349	338.915	1129.716	4.482	49.802	3.000	0.600	19.000	34.200
	s11	220.216	367.026	1223.419	4.854	53.932	2.000	0.600	30.650	36.780
	s14	230.979	384.965	1283.216	5.091	56.568	1.000	0.600	65.267	39.160

$$Ag = \beta * e^{\alpha * \frac{Mu}{d}} = N * L * T_{ult} \quad (1)$$

In the context of the provided information, the variables in the equation have specific meanings. The symbol Ag represents the total ultimate strength of the uniaxial geogrid on the footing in (kN). Mu represents the ultimate moment exerted on the footing in (kN. 0.60 m), while d corresponds to the depth of the strip footing in (m).

The constants β and α are specific values that depend on the concrete mixture used in the tested footing specimens. For reinforced concrete mixture, the values of β and α are 14.178 and 0.0186, respectively.

For glass fiber reinforced concrete (GFRC), the values of β and α are 13.249 and 0.0193, respectively. The variable N represents the number of geogrid layers, L represents the length of geogrid within the footing in meters (m), and T_{ult} represents the tensile strength of the uniaxial geogrid used, measured in kilonewtons per meter (kN/m)

3.6 Economical Study for Strip footings Reinforcement.

This point explores the impact of various uniaxial geogrid reinforcements with added glass fiber bristles on the load capacity of strip footings. In Table 6, a detailed breakdown of reinforcement costs is provided, including the calculated percentage changes in prices compared to St1. For a visual representation of the relationship between the rise in reinforcement price ratio and the corresponding increases in load ratios at various stages, refer to Fig. 16. The result can be summarized as follows:

- **Single Layer of Re 580 Geogrid:**

Utilizing a single layer of Re 580 geogrid as the main reinforcement led to significant improvements: the first crack load, yield load, and ultimate load increased by 42.22%, 111.96%, and 106.21%, respectively, alongside a cost increase of 120.35%.

- **Double Layer of Re 540 Geogrid:**

Incorporating two layers of Re 540 geogrid as the main reinforcement resulted in noteworthy enhancements: the first crack load, yield load, and ultimate load rose by 37.78%, 97.04%, and 96.60%. The cost also increased by 110.84%.

- **Triple Layer of Re 510 Geogrid:**

The use of three layers of Re 510 geogrid as the main reinforcement demonstrated improvements in the first crack load, yield load, and ultimate load by 23.33%, 73.25%, and 81.54%, respectively, with a corresponding cost increase of 129.83%.

- **Single Layer of Re 570 Geogrid:**

Applying a single layer of Re 570 geogrid as the main reinforcement resulted in a 22.22% enhancement in the first crack load, a 60.72% increase in the yield load, and a 68.02% improvement in the ultimate load. The associated cost increase was 82.36%.

- **Double Layer of Re 520 Geogrid:**

Using two layers of Re 520 geogrid as the main reinforcement led to increased load-bearing capacity: the first crack load, yield load, and ultimate load increased by 16.67%, 48.58%, and 51.87%, respectively. This approach also incurred a cost increase of 87.59%.

- **Single Layer of Re 560 Geogrid:**

Interestingly, a single layer of Re 560 geogrid as the main reinforcement contributed to load improvements: the first crack load, yield load, and ultimate load increased by 13.33%, 30.33%, and 28.02%, respectively, while increased the cost by 47.47%.

Table 6: Percentage Change in Reinforcement Prices Compared to St1.

Reinforcement material	**No. of layers**	**Footing Number**	**Ratio increases on $P_{f.c}$ %**	**Ratio increases on P_y %**	**Ratio increases on P_u %**	**Total Price of specimen (E.G.P)**	**Change on Ratio price (%)**
Steel		St1	-			37.92	-
All footings compared to control footing (St1)							
Re 560	one	St12	13.33%	30.07%	28.02%	55.92	47.47%
Re 520	Two	St10	16.67%	48.58%	51.87%	71.14	87.59%
Re 570	one	St13	22.22%	60.72%	68.02%	69.15	82.36%
Re 510	Three	St9	23.33%	73.25%	81.54%	87.15	129.83%
Re 540	Two	St11	37.78%	97.04%	96.60%	79.95	110.84%
Re 580	one	St14	42.22%	111.96%	106.21%	83.56	120.35%

This means that to reach the best result, the designer must choose the geogrid needed to resist the stresses while reducing the number of uniaxial geogrid layers as much as possible. This is because increasing the number of layers to resist stresses and bending moments increases the economic cost. Therefore, Footing St12, reinforced with one layer of geogrid, Re 560, can be considered the best and lowest increments footing at the same time.

The cost of the control footing has decreased because the amount of steel reinforcement used in the footing is lower in comparison to the cost of using geogrid reinforcement.

Moreover, the enhancement in load-bearing capacity achieved through geogrid reinforcement has become evident. This advancement is expected to allow for the use of smaller geogrid sheets, leading to significant cost savings while still achieving a performance level comparable to that of steel reinforcement.

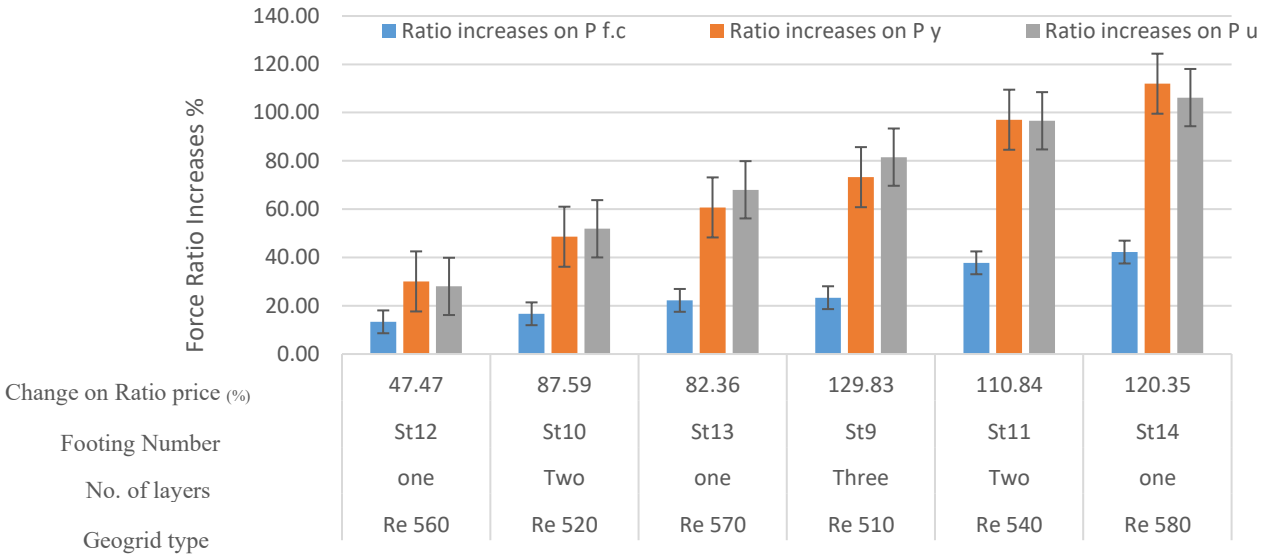

Fig. 16: Relationship Between Price Ratio Escalation due to Reinforcement and specimen Number for Tested Strip footing specimens

IV. CONCLUSION

1- Incorporating uniaxial geogrid reinforcement into strip footing significantly enhances load capacities. P_{fc}, P_y, and P_{ult} experience substantial increases compared to the control footing, primarily due to the increased tensile strength from the geogrid reinforcement.

2- Using uniaxial geogrid reinforcement on strip footing significantly bolsters footing stiffness during first crack and yield stages, yet elongation of geogrid leads to subsequent fragility and weakening in the ultimate stage for footings.

3- Uniaxial geogrid reinforcement substantially improves strip footing performance, enhancing both displacement ductility and energy dissipation capacities compared to control footings. The extent of improvement varies depending on the geogrid's tensile strength, with a positive correlation to geogrid stiffness and tensile strength.

4- Glass fiber bristles with Uniaxial geogrid reinforcement, particularly Re 510, Re 520, Re 540, Re 560, Re 570, and Re 580, consistently enhance strip footing performance. These enhancements result in increases for P_{fc}, P_y, and P_{ult} compared to the concrete control strip footing (St1).

5- Incorporating glass fiber bristles along with uniaxial geogrid reinforcement uniformly enhances the stiffness of strip footing performance. This approach results in notable enhancements for k_{fc}, k_y, and k_{ult} compared to the concrete control strip footing (St1).

6- Combining uniaxial geogrid reinforcement with glass bristles on strip footings consistently enhances performance. This improvement correlates with the total tensile strength of the reinforcement, impacting displacement ductility indexes and energy dissipation capacities affirmatively.

7- The integration of uniaxial geogrid with concrete prominently contributed to decrease both crack thickness and quantity. geogrid reinforced footings exhibited a notable correlation between the number of flexural cracks, total geogrid tensile strength, and the number of geogrid layers.

8- An empirical equation linking strip footing moment and total tensile strength of geogrid reinforcements was derived.

9- Through careful sheet selection and layers reduction, Strip footing load capacity is enhanced, outperforming traditional steel methods.

REFERENCES

[1] Tharani, K., Mahendran, N., & Vijay, T. J. (2019). Experimental investigation of geogrid reinforced concrete slab. International Journal of Innovative

Technology and Exploring Engineering, 8(6), 88-93.

[2] Banu, S. T., Chitra, G., Awoyera, P. O., & Gobinath, R. (2019). Structural retrofitting of corroded fly ash based concrete beams with fibres to improve bending characteristics. Australian Journal of Structural Engineering.

[3] El-Kasaby, E. S. A., Roshdy, M., Awwad, M., & Abo-Shark, A. A. (2023). Enhancing Flexural Performance of GFRC Square Foundation Footings through Uniaxial Geogrid Reinforcement. International Journal of Advanced Engineering, Management and Science, 9, 8.

[4] El-Kasaby, E. S. A., Awwad, M., Roshdy, M., & Abo-Shark, A. A. (2023). Behavior of Square footings reinforced with glass fiber bristles and biaxial geogrid. European Journal of Engineering and Technology Research, 8(4), 5-11.

[5] Hadi MNS, Al-Hedad ASA (2020) Flexural fatigue behaviour of geogrid reinforced concrete pavements. Constr Build Mater 249:118762.

[6] Meng X, Chi Y, Jiang Q, Liu R, Wu K, Li S (2019) Experimental investigation on the flexural behavior of pervious concrete beams reinforced with geogrids. Constr Build Mater 215:275–284.

[7] Tang, Xiaochao, Isaac Higgins, and Mohamad N. Jlilati. "Behavior of Geogrid-Reinforced Portland Cement Concrete under Static Flexural Loading." Journal of Materials in Civil Engineering, vol. 31, no. 3, 2019, pp. 04018399.

[8] Jallu M, Arulrajah A, Saride S, Evans R (2020) Flexural fatigue behavior of fly ash geopolymer stabilized-geogrid reinforced RAP bases. Constr Build Mater 254:119263.

[9] Chen C, McDowell GR, Thom NH (2014) Investigating geogrid- reinforced ballast: experimental pull-out tests and discrete ele- ment modelling. Soils Found 54:1–11.

[10] Abdesssemed, M., Kenai, S. and Bali, A.," Experimental and Numerical Analysis of the Behavior of an Airport Pavement Reinforced by Geogrids," Constrtruction. and Building Materials. 2015, Vol. 94, no. 5, pp 547–554

[11] Tang, X., Higgins, I. and N Jlilati, M. (2018). Behavior of Geogrid Reinforced Portland Cement Concrete under Static Flexural Loading. Infrastructures, 3(4), 41.

[12] Maxwell, S., Kim, W., Edil, T. B., and Benson, C.H. (2005). Effectiveness of Geosynthetics in Stabilizing Soft Subgrades. Report to the Wisconsin Department of Transportation.

[13] Webster, S.L. (1993). Geogrid Reinforced Base Course for Flexible Pavements for Light Aircraft, Test section Construction, Behavior under Traffic, Laboratory Test Design Criteria. Technical Report GL-93-6, U.S. Army Corps of Engineers, Waterways Experiment Station, Viksburg, MS, USA.

[14] Qian, Y. (n.d.). Experimental Study on Triangular Aperture Geogrid-Reinforced Bases over Weak Subgrade under Cyclic Loading. Retrieved May 1, 2010, from http://www.geocon.net/pdf/paper28.pdf.

[15] Tang, X., Palomino, A., and Chehab, G.R. (2008). Laboratory Evaluation of Geogrids for Flexible Pavement Reinforcement. In The First Pan American Geosynthetics Conference and Exhibition, GeoAmericas 2008 Conference Proceedings, International Geosynthetics Society.

[16] Tang, X., Chehab, G. R., and Kim, S. (2008). Laboratory Study of Geogrid Reinforcement in Portland Cement Concrete. In Pavement Cracking Mechanisms, Modeling, Detection, Testing, and Case Histories (pp. 769- 778). Al-Qadi, Scarpas, and Loizos (Eds.), Taylor& Francis Group.

[17] Abdelmonem Mohamed, R. N., El Sebai, A. M., and Gabr, A. S. A. H. (n.d.). Flexural Behavior of Reinforced Concrete Slabs Reinforced with Innovative Hybrid Reinforcement of Geogrids and Steel Bars. Canadian Geotechnical Journal. doi: 10.1139/cgj-2022-0112

[18] El Meski, F., and Chehab, G. (2014). Flexural Behavior of Concrete Beams Reinforced with Different Types of Geogrids. Journal of Materials in Civil Engineering, 26(8), 04014038.

[19] Radnic, J., Matesan, D., Grgic, N., and Baloevic, G. (2015). Impact testing of RC slabs strengthened with CFRP strips. Composite Structures, 121, 90-103. doi: 10.1016/j.compstruct.2014.11.032

[20] Gabr, A. S. A. H. (2019). Strengthening of Reinforced of Concrete Slabs Using Different Types of Geo-grids. International Journal of Civil Engineering and Technology (IJCIET), 10(1), 1851-1861.

[21] El Meski, F., and Chehab, G. R. (2014). Flexural behavior of concrete beams reinforced with different types of geogrids. Journal of Materials in Civil Engineering, 26(8), 04014038.

[22] Tam AB, Park D-W, Le THM, Kim J-S (2020) Evaluation on fatigue cracking resistance of fiber grid reinforced asphalt concrete with reflection cracking rate computation. Constr Build Mater 239:117873.

[23] Pant A, Datta M, Ramana GV, Bansal D (2019) Measurement of role of transverse and longitudinal members on pullout resistance of PET geogrid. Measurement 148:106944.

[24] Tahir M, Wang Z, Ali KM, Isleem HF. Shear behavior of concrete beams reinforced with CFRP sheet strip stirrups using wet-layup technique. Structures. 2019;22:43–52.

[25] Ali B, Qureshi LA. Influence of glass fibers on mechanical and durability performance of concrete with recycled aggregates. Constr Build Mater 2019;228:116783. https://doi.org/10.1016/j.conbuildmat.2019.116783.

[26] Siva Chidambaram R, Agarwal P. The confining effect of geo-grid on the mechanical properties of concrete

specimens with steel fiber under compression and flexure. Constr Build Mater 2014;71:628–37.

[27] Tensar International Corporation and imported, 2500 Northwinds Parkway, Suite 500 Alpharetta, GA 30009, Tel. (770) 344-2090 Email: info@tensarcorp.com, web. https://www.tensarcorp.com/solutions/geogrids/triax.

[28] ECP-Egyptian Code of Practice-201, "Egyptian code of practice" no. 201 for calculating loads and forces in structural work and masonry, National Research Center for Housing and Building, Ministry of Housing, Utilities and Urban Planning, Cairo, 2011

[29] Meski F, Chehab G. Flexural behavior of concrete beams reinforced with different types of geogrids. J Mater Civil Eng 2013;26(8):04014038.

[30] Meng, X., Zhang, M., & Liu, S. (2019). Investigation of the mechanical properties of pervious concrete beams reinforced with biaxial geogrids. Construction and Building Materials, 198, 92-102. doi: 10.1016/j.conbuildmat.2018.11.118

[31] Susumu, I. (1994). Ductility and Energy Dissipation of Concrete Beam Members and Their Damage Evaluation Based on Hysteretic Dissipated Energy (Doctoral dissertation). Kyoto University, Kyoto, Japan.